



# CHORUS

This is the accepted manuscript made available via CHORUS. The article has been published as:

## Spatiotemporal patterns emerging from a spatially localized time-delayed feedback scheme

Jason Czak and Michel Pleimling

Phys. Rev. E **104**, 064213 — Published 20 December 2021

DOI: [10.1103/PhysRevE.104.064213](https://doi.org/10.1103/PhysRevE.104.064213)

# Spatio-temporal patterns emerging from a spatially localized time-delayed feedback scheme

Jason Czak<sup>1,2,\*</sup> and Michel Pleimling<sup>1,2,3</sup>

<sup>1</sup>*Department of Physics, Virginia Tech, Blacksburg, VA 24061-0435, USA*

<sup>2</sup>*Center for Soft Matter and Biological Physics,  
Virginia Tech, Blacksburg, VA 24061-0435, USA*

<sup>3</sup>*Academy of Integrated Science, Virginia Tech, Blacksburg, VA 24061-0563, USA*

(Dated: December 2, 2021)

## Abstract

In attempts to manage spatio-temporal transient chaos in spatially extended systems, these systems are often subjected to protocols that perturb them as a whole and stabilize globally a new dynamic regime, as for example a uniform steady state. In this work we show that selectively perturbing only part of a system can generate space-time patterns that are not observed when controlling the whole system. Depending on the protocol used, these new patterns can emerge either in the perturbed or the unperturbed region. Specifically, we use a spatially localized time-delayed feedback scheme on the one-dimensional Gray-Scott reaction-diffusion system in the transient chaotic regime and demonstrate, through the numerical integration of the resulting kinetic equations, the stabilization of spatially localized space-time patterns that can be perfectly periodic. The mechanism underlying the observed pattern generation is related to diffusion across the interfaces separating the perturbed and unperturbed regions.

---

\*Electronic address: [jec5103@vt.edu](mailto:jec5103@vt.edu)

## I. INTRODUCTION

Spatio-temporal patterns [1, 2] are ubiquitous in nature and are found at scales ranging from the very small, bacterial colonies [3] and developmental biology [4], to the very large, as for example galaxy superclusters [5] or the Sloan Great Wall [6]. The spontaneous formation of patterns, a hallmark of systems far from equilibrium, has captivated the interest of researchers from a vast variety of disciplines. Common to many mechanisms yielding space-time patterns is the closeness to an instability (for example a chemical or hydrodynamics instability). Chemical reaction-diffusion systems [7] have been at the center of the investigations of pattern formation since Turing's seminal work [8], as they underpin many phenomena observed in nature and allow for both numerical and analytical approaches when cast in terms of coupled partial differential equations. Very rich space-time patterns, from chemical oscillations and Turing patterns [9] to spatio-temporal chaos [10], can be found in reaction-diffusion systems in open flow reactors that keep the systems far from equilibrium.

Controlling and designing space-time patterns has many potential applications. The goal is often either to design patterns and influence traveling waves [12–16] or to move a chaotic system to a steady state or to an oscillatory behavior [18–24]. Experimentally, this control is achieved by exerting some external perturbation, involving for example photochemical energy transfer or temperature variations when dealing with chemical systems. Successful control protocols include the Ott-Grebogi-Yorke scheme [18] as well as time-delayed feedback control [19].

In this work we demonstrate that new space-time patterns can be generated in systems with (transient) chaos when using spatially localized invasive perturbations in the form of a time-delayed feedback scheme applied to a specified region of the system. We illustrate this through the creation in the one-dimensional Gray-Scott model of novel spatially localized time-dependent patterns. Our work differs both in the goals and in the scheme from other studies aiming at control of (transient) chaos in a spatially extended system. For example, in [23] time-delayed feedback control was used in order to control the transient chaos [10] regime and replace it in the whole system with other types of dynamic behavior, whereas for the pinning control of spatio-temporal chaos [25], a finite number of spatial pinning sites, arranged in optimal ways, are controlled in order to drive the whole system into a homogeneous steady state. Controlling the whole system or a finite number of specially

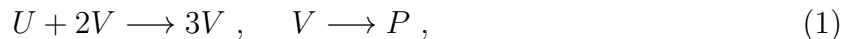
arranged pinning sites does not result in the formation of new space-time patterns in a specified spatial region.

One remarkable finding of our work is that patterns can be stabilized locally that have periods orders of magnitude longer than the delay time used for the spatially localized perturbations. This is very different to reported [26–28] stabilizations of complex spatio-temporal dynamics near a subcritical Hopf bifurcation using global feedback control as for these systems the time delay is a multiple of the period of the newly stabilized periodic pattern. In our systems with spatially localized perturbations it is the interplay between time delay and spatial boundaries separating perturbed and unperturbed regions that generates the long-period patterns discussed in the following study.

In Section II we briefly remind the reader about some relevant aspects of the Gray-Scott model before discussing the application of time-delayed feedback scheme to this type of reaction-diffusion systems. Section III presents the novel space-time patterns that emerge when applying in the chaotic regime the time-delayed feedback scheme to part of the system only. Two scenarios are discussed, leading in one case to perfect periodic patterns, whereas in the other case the pattern is impacted by noise generated from diffusion across the boundaries separating the perturbed and unperturbed regions. In Section IV we conclude and provide an outlook on broader applications of the scheme discussed in this paper.

## II. MODEL AND METHOD

The Gray-Scott model [29] is a reaction-diffusion system that displays very rich and complex space-time patterns in one [30–35] and two [36–38] space dimensions. This cubic autocatalytic system in an open flow reactor is governed by the reactions



where the substrate  $U$  is continuously supplied and the inert product  $P$  is removed. The corresponding deterministic kinetic equations for the space- and time-dependent species concentrations  $u(\mathbf{x}, t)$  and  $v(\mathbf{x}, t)$  are often cast in the form

$$\frac{\partial u}{\partial t} = D_u \nabla^2 u - uv^2 + A(1 - u) \quad (2)$$

$$\frac{\partial v}{\partial t} = D_v \nabla^2 v + uv^2 - (A + B)v \quad (3)$$

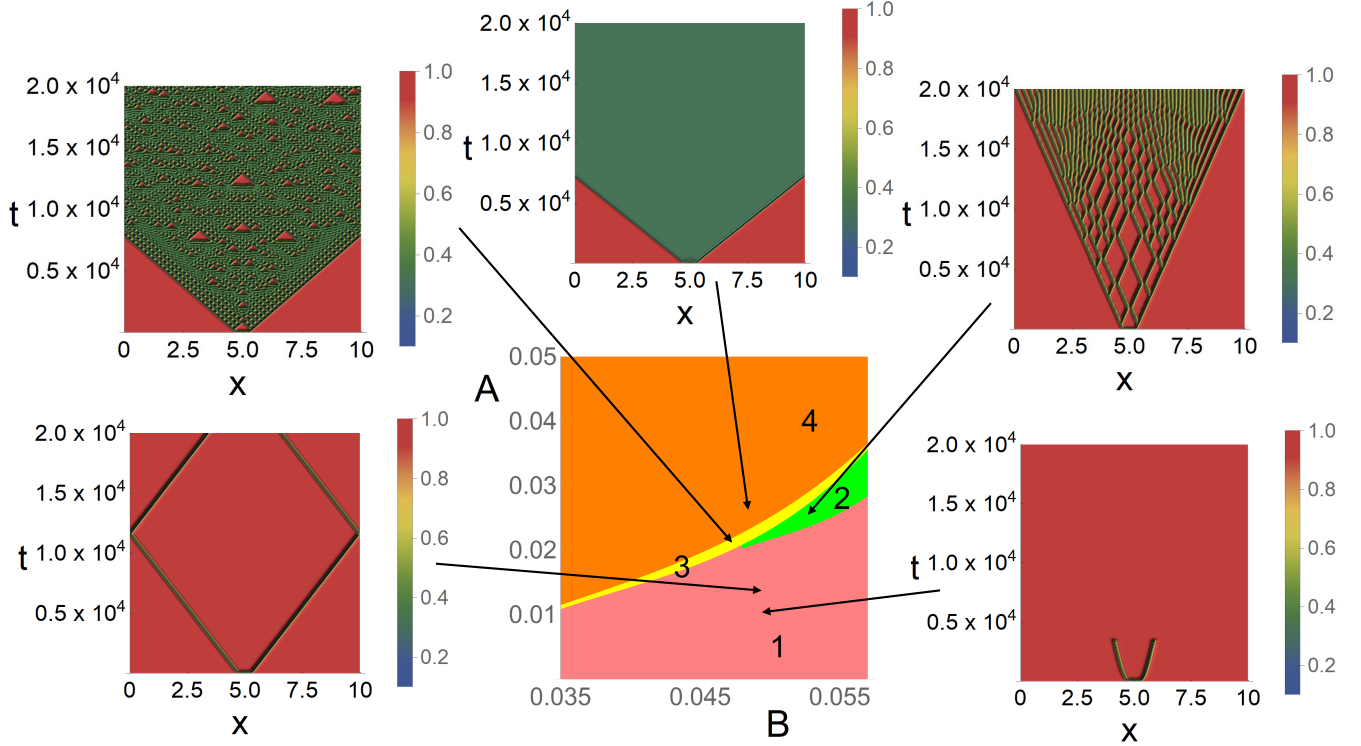


FIG. 1: The different dynamic regimes encountered for  $D_u/D_v = 2$ , with  $D_u = 2 \times 10^{-5}$  and  $D_v = 10^{-5}$ , and an inhomogeneous initial state with  $(u, v) = (0.5, 0.25)$  in a small central region and  $(u, v) = (1, 0)$  otherwise. Space-time plots for  $u$  are obtained through numerical integration of the discretized versions of Eqs. (2) and (3), using periodic boundary conditions. The time increment is chosen as  $\Delta t = 0.05$ . The width of the system is  $L = 10$ , and 1024 grid points are used for the spatial discretization.

with the species-dependent diffusion rates  $D_u$  and  $D_v$  as well as the rate  $B$  of converting  $V$  into the inert product and the rate  $A$  of feeding  $U$  into the reactor and of removing the different species from the reactor. Whereas for  $D_u \gg D_v$  propagating pulses and pulse splittings dominate, for  $D_u \gtrsim D_v$  a variety of regimes, including traveling pulses, spatio-temporal chaos, and self-replicating patterns, are encountered, depending on the values of the rates  $A$  and  $B$ .

In this work we restrict ourselves to the ratio  $D_u/D_v = 2$  which is known to yield (transient) chaotic space-time patterns as a result of an inhomogeneous initial state. We follow previously published work and select as initial state the state with  $(u, v) = (0.5, 0.25)$  in a small central region and  $(u, v) = (1, 0)$  everywhere else. The resulting dynamic phase

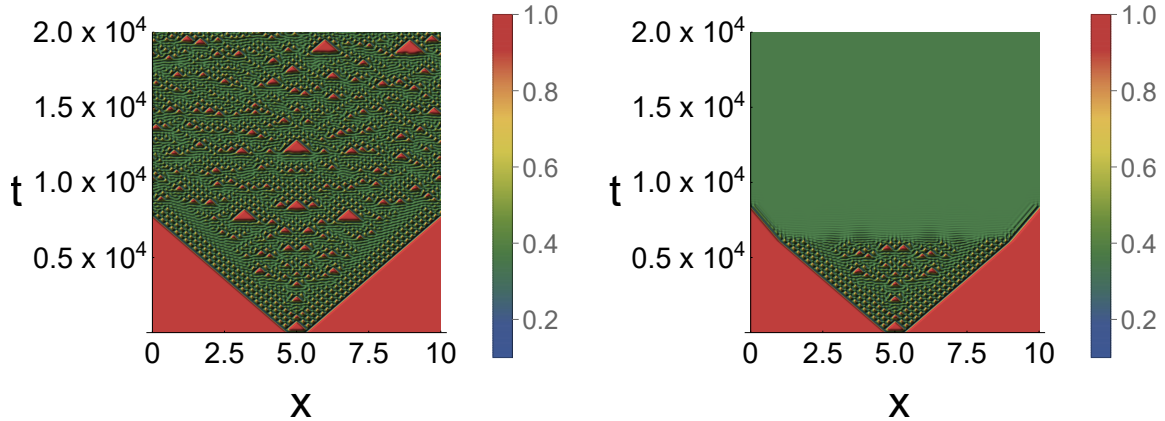


FIG. 2: (Left) Spatio-temporal chaos in the one-dimensional Gray-Scott model that results from an inhomogeneous initial state. Shown is  $u(x, t)$ . The parameters are  $D_u/D_v = 2$ ,  $A = 0.0234$ , and  $B = 0.05$ . The initial state is  $(u, v) = (1, 0)$ , with the exception of the region in the middle where  $(u, v) = (0.5, 0.25)$ . (Right) When controlling the whole system using time-delayed feedback control, spatio-temporal chaos is suppressed and a non-trivial steady state with  $u \neq 0$  and  $v \neq 0$  can be stabilized [23]. The perturbation, which starts at  $t = 6,000$ , is characterized by the strength  $K = -0.02$  and the delay time  $\tau = 0.5$ .

diagram and the corresponding space-time plots for  $u$  are shown in Fig. 1. Regime 1 is characterized by individual traveling pulses that either die out quickly, yielding the trivial steady state  $(u, v) = (1, 0)$ , or continue to propagate. In regime 2, pulse splitting results in the generation of additional lines and the formation of domains that evolve temporally. Regime 3 is the transient chaotic regime that results from the interaction between a Hopf instability and a Turing instability [31–33]. This transient chaotic regime, which sees the appearance and disappearance of small regions where the densities  $u$  and  $v$  take on values close to those of the trivial steady state, is confined to a rather narrow region in parameter space. Finally, for large inflow rates  $A$  the system settles into a non-trivial steady state with  $u \neq 0$  and  $v \neq 0$  (regime 4).

The left panel in Fig. 2 shows more clearly the transient chaotic regime that emerges for  $D_u/D_v = 2$ ,  $A = 0.0234$ , and  $B = 0.05$ . The controlled patterns obtained in [23], where time-delayed feedback control was applied to the system as a whole, included a non-trivial steady state with  $u \neq 0$  and  $v \neq 0$ , shown in the right panel of Fig. 2 for the same parameter values as for the left panel, as well as coarsening patterns and traveling waves. As discussed

in the following, when applying a time-delayed feedback scheme to only parts of the system, spatially localized ordered patterns can be stabilized. These patterns are not encountered when controlling the whole system [23].

In our protocol of perturbing the substrate in a spatially localized way, Eq. (2) is replaced in some region  $\mathcal{C}$  with [39]

$$\begin{aligned} \frac{\partial u(\mathbf{x}, t)}{\partial t} = & D_u \nabla^2 u(\mathbf{x}, t) - u(\mathbf{x}, t)v(\mathbf{x}, t)^2 + A(1 - u(\mathbf{x}, t)) \\ & + K (u(\mathbf{x}, t - \tau) - u(\mathbf{x}, t)) \end{aligned} \quad (4)$$

with the perturbation strength  $K$  and the delay time  $\tau$ . We present below numerical results for the value  $\tau = 0.5$ . When the region  $\mathcal{C}$  is the whole system, we of course recover the situation studied in [23].

Kyrychko et al. [23] pointed out that the effective perturbation strength is  $|K|\tau$  when this scheme is applied to the system as a whole. In our work we perturb the system only locally, and, while the effective control strength is still provided by  $|K|\tau$ , different local patterns are stabilized depending on the sign of  $K$ . As a result, additional constraints are imposed on the values of the delay time for which these patterns can be stabilized. For  $K = -0.03$ , which is the negative value we focus on in the following, periodic patterns are stabilized in the unperturbed region for  $0.45 < \tau < 1.75$ . For  $K = 0.025$ , the positive value explored later in this work, we observe the appearance of approximate periodic patterns for a very wide range of delay times, with  $0.45 < \tau < 10$ , where  $\tau = 10$  is the longest delay time that we investigated.

Applying periodic boundary conditions, the discretized versions of the differential equations given above are integrated using the fourth order Runge-Kutta algorithm and an eight order finite difference method for the diffusion terms. This results in a very stable integration scheme. Still, the symmetry imposed by the initial condition used for Fig. 2 is lost in the chaotic regime at very long times (for  $t$  of the order of  $1.5 \times 10^4$  in the left panel of Fig. 2) due to the accumulation of numerical errors. We checked that the loss of right-left symmetry sets in much earlier when using a lower order discretization of the diffusion term.

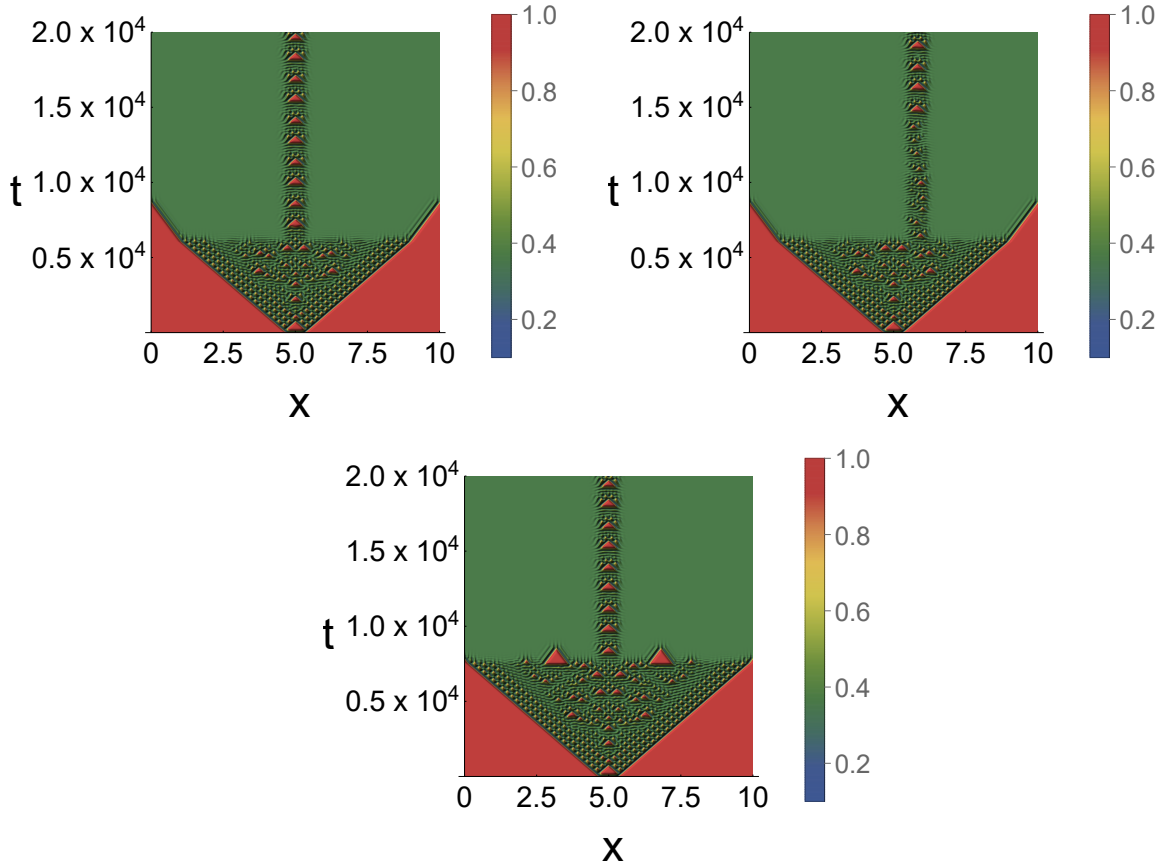


FIG. 3: (Top left) Using time-delayed feedback for species  $U$  everywhere in the system with the exception of the central region of width  $W_{un} = 0.625$  induces a periodic pattern in the *unperturbed* region. The period of the resulting oscillations in the unperturbed region is many orders of magnitude larger than the delay time  $\tau = 0.5$ . For this plot the strength  $K = -0.03$  was used and the perturbation started at  $t = 6,000$ . (Top right) The same as in the top left panel, but now the unperturbed region has been shifted by 0.83 to the right when compared to the case on the left. The time needed to establish the periodic pattern depends on the state of the system at the location of the unperturbed region just before the localized time-delayed feedback scheme sets in. (Bottom) The same as in the top left panel, but now with the perturbation starting at  $t = 7,500$ . Even so the state at the onset of the perturbation differs from that at  $t = 6,000$ , the same periodic pattern is stabilized. For all figures the parameter values are  $D_u/D_v = 2$ ,  $A = 0.0234$ , and  $B = 0.05$ .

### III. RESULTS

The two scenarios discussed in the following for the one-dimensional Gray-Scott model have in common that we let the system shown in the left panel of Fig. 2 evolve for some time and then perturb in a specified region the substrate using time-delayed feedback. For the first case discussed below, we show that applying a perturbation to a broad region the system with  $K < 0$  may yield in the *unperturbed* region a perfectly periodic pattern. On the other hand, if the feedback strength parameter is positive,  $K > 0$ , then noisy repeating patterns can be stabilized in the *perturbed* region, where the noise results from diffusion across the boundary separating the perturbed from the unperturbed, and therefore chaotic, region.

#### A. $K < 0$

As shown in the right panel of Fig. 2, controlling the whole system with  $K < 0$  results in the suppression of spatio-temporal chaos everywhere and in the global stabilization of the non-trivial steady state. This is the only non-chaotic regime that can be stabilized globally for negative  $K$  [23]. Restricting this protocol to a part of the system suppresses chaos only locally so that this non-trivial steady state is not established everywhere. Instead, as shown in the top left panel of Fig. 3, in the unperturbed region the system spontaneously organizes into a perfectly periodic structure, dominated by periodically appearing space-time regions, shown as red triangles, where the trivial steady state  $(u, v) = (1, 0)$  is approximated. This periodic pattern has a remarkably long period  $T \approx 2,700$ , almost four orders of magnitude larger than the delay time  $\tau = 0.5$  used in the feedback. Inspection of the time-dependent species concentration  $u$  in the middle of the unperturbed region, see Fig. 4, reveals that within one period the concentration  $u$  displays two pronounced maxima, corresponding to two red triangles in the space-time plot. As shown in Fig. 5 the amplitude  $|a_u|$  of the Fourier transform of  $u(t)$  in this part of the system also reveals this complex periodic pattern and exhibits as a function of the frequency  $f$  sharp peaks at the relevant frequencies.

The emergence of this periodic pattern is independent of the location of the unperturbed region. The top right panel in Fig. 3 shows that the same structure emerges when the unperturbed region is off-center. However, the time needed to establish the pattern can

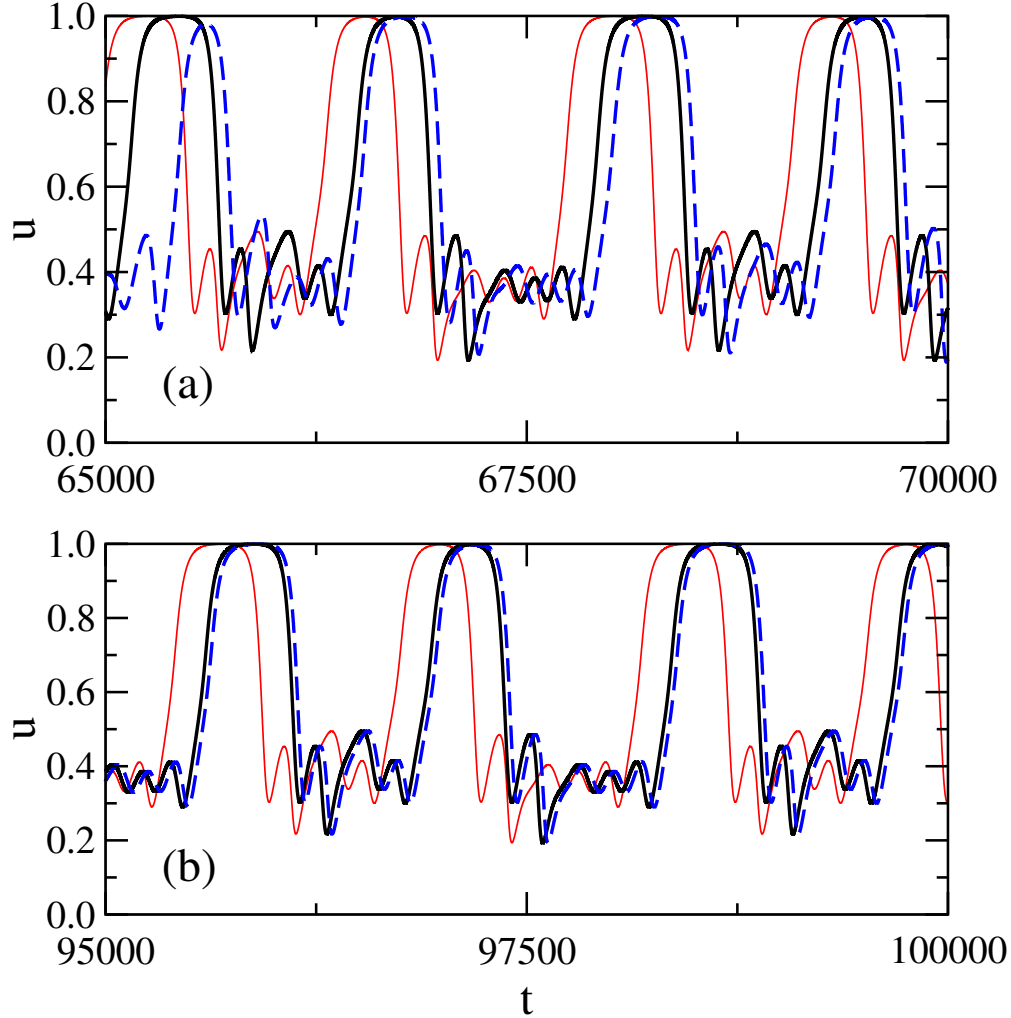


FIG. 4: Time-dependent concentration  $u$  in the middle of the unperturbed region for the three perturbation times  $t_p = 6,000$  (black lines),  $t_p = 7,500$  (red lines), and  $t_p = 60,000$  (dashed blue lines), see top left and bottom panels in Fig. 3 for the corresponding space-time plots: (a)  $t$  between 65,000 and 70,000; (b)  $t$  between 95,000 and 100,000. When applying the time-delayed feedback outside of the middle region, the species concentration after some transient behavior (visible for  $t_p = 60,000$  in panel (a)) locks into a periodic pattern with a period  $T \approx 2,700$ . This periodic pattern, once established, is independent of the perturbation time, the only difference being an overall time shift as the periodic pattern sets in at different times for the different perturbation times. The parameters used in this figure are the same as in Fig. 3.

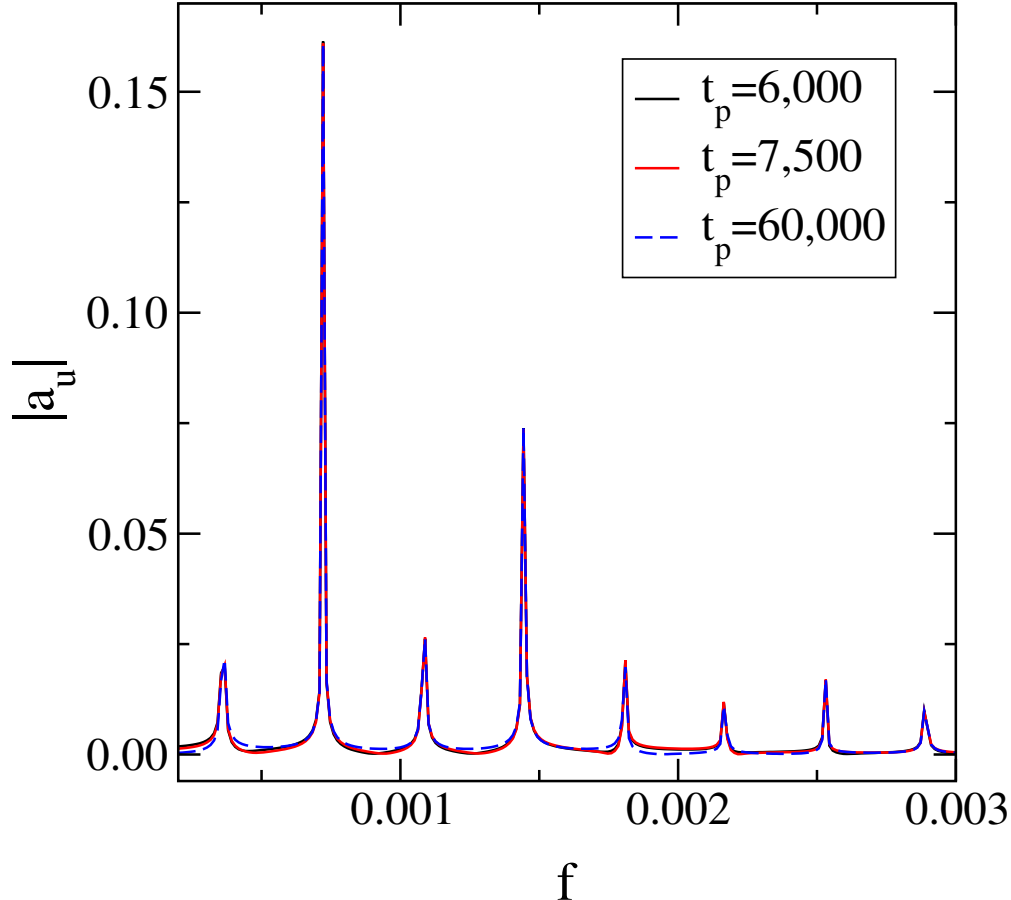


FIG. 5: Frequency-dependent amplitude of the Fourier transform of the time-dependent concentration  $u$  in the middle of the unperturbed region of width  $W_{un} = 0.625$ , see Fig. 4 for the corresponding time series. The very sharp peaks in the Fourier transform indicate that within the unperturbed region the pattern is repeated perfectly. The shown data for three different perturbation times ( $t_p = 6,000$ ,  $t_p = 7,500$ , and  $t_p = 60,000$ ) exhibit the same prevailing frequencies, as revealed by the identical positions of the peaks. This indicates that the emerging periodic pattern is robust and independent of the perturbation time.

vary substantially, which reveals a dependence on the state of the unperturbed region at the moment the perturbation sets in. The width  $W_{un}$  of the unperturbed region is a relevant quantity, as the perfect periodic pattern is not observed for all widths of the unperturbed region. Indeed, for  $W_{un} \gtrsim 1.1$ , the unperturbed region maintains the chaotic property of the original system. On the other hand, if  $W_{un} \lesssim 0.2$ , spatial and temporal inhomogeneities die out in the unperturbed region and the system as a whole is pushed into the non-trivial steady state. The range of widths  $W_{un}$  of the unperturbed region for which periodic patterns

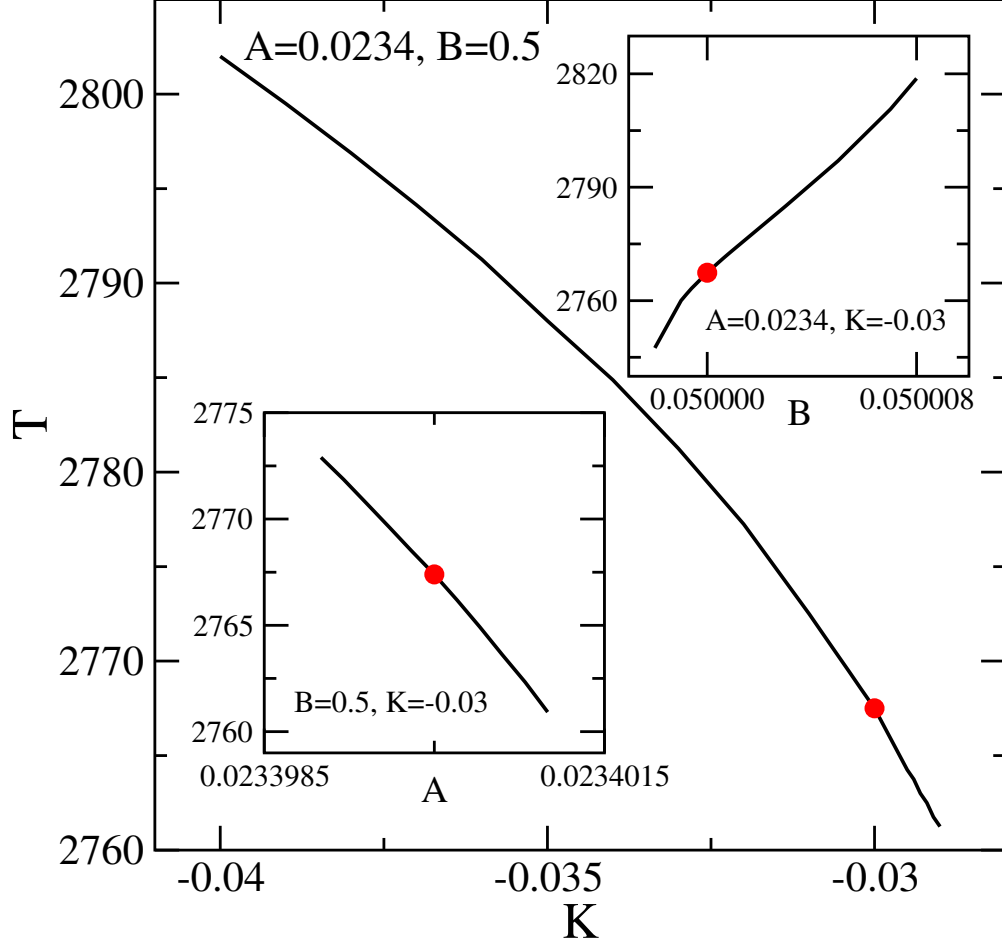


FIG. 6: Dependence of the period  $T$  of the repeating pattern when changing the feedback strength  $K$  (main image), the flow rate  $A$  (lower left inset) or the rate  $B$  of converting  $V$  into an inert product (upper right inset). We explore the parameter range around the values  $K = -0.03$ ,  $A = 0.0234$ , and  $B = 0.5$ , used in the Figs. 3, 4, and 5, and indicated by the red dot in each panel. For each plot, two parameters are kept constant, as indicated in the panels, and the third is varied. As for the earlier figures,  $D_u/D_v = 2$ , whereas the width of the unperturbed region is  $W_{un} = 0.625$ .

can be induced is independent of the linear extent of the system.

We also remark, see the bottom panel in Fig. 3 as well as the corresponding time-dependent concentration in Fig. 4, that the emerging pattern is independent of the perturbation time itself (provided that chaotic behavior is present when the perturbation sets in). This is clearly visible in Fig. 4 when comparing the time-dependent concentrations for different perturbation times. The observed overall time shift is a consequence of the fact that the periodic patterns set in at different times for the different situations.

Fig. 6 explores how the period  $T$  of the repeating pattern changes when the system parameters are changed. In the main image we show the period as function of the feedback strength  $K$ , keeping the other parameters constant at the values used for Figs. 3, 4, and 5. In the two insets, we show how the period changes when varying the flow rate  $A$  (lower left inset) or the rate  $B$  to produce the inert product (upper right inset), while keeping all other parameters constant. These plots also provide an indication of the extent to which the parameters can be varied around our standard set  $K = -0.03$ ,  $A = 0.0234$ , and  $B = 0.5$  while still generating a periodic pattern. Increasing the rate  $B$  yields a substantial increase of the period. On the other hand changing the flow rate  $A$  yields changes in the form of an approximate linear decrease for increasing  $A$ . Keeping  $A$  and  $B$  constant while merely changing the value of  $K$  means that any change to the period is exclusively due to the details of the feedback scheme. It is then interesting to note that an increase of the magnitude of  $K$  increases the time between successive repetitions of the pattern. We also remark that values  $|K| < 0.028$  do not allow to stabilize the periodic pattern, but that instead chaotic patterns persist in the unperturbed region. On the flip side, large negative values, with  $K < -0.042$ , tend to destabilize the periodic pattern, once established, resulting in an intermittent behavior where time intervals with repeating patterns are interrupted by time intervals where the behavior is no longer fully periodic. Therefore outside of the interval  $-0.042 < K < -0.028$  no period can be measured due to the absence of repeating patterns.

At first look it might seem that the periodic pattern emerging in the unperturbed region is mainly a consequence of exposing a region of the right size to a fixed boundary condition provided by the adjacent steady-state region. A closer inspection, however, reveals that the feedback scheme is the necessary ingredient to generate periodic patterns. This is illustrated in Fig. 7 for the system with our standard parameters. With the feedback scheme in place, the pattern remains perfectly periodic for as long as we follow the time evolution of the system (left panel). In the right panel, we remove the time-delayed feedback (by setting  $K = 0$ ) at  $t = 25,000$ , indicated by the dashed horizontal line. Without the continuous application of the time-delayed feedback, the periodic pattern is immediately lost and replaced by the random appearance of small red triangles in the space-time plot. The absence of periodic pattern is also noted in Fig. 8 where instead of switching on the time-delayed feedback scheme at  $t = 6,000$  we make in the same region an instantaneous change of  $A$  from 0.0234 to 0.03, a value for which an unperturbed system settles into the global non-trivial steady

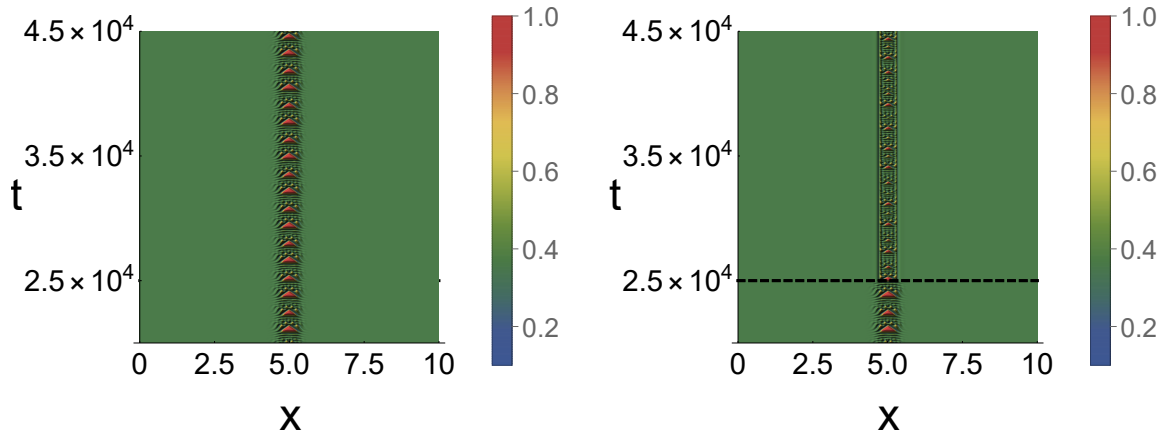


FIG. 7: (Left) The same system as in the left panel of Fig. 2 in the time interval between  $t=20,000$  and  $t=45,000$ . (Right) The same system, but now with the time-delayed feedback switched off at  $t = 25,000$ , indicated by the dashed line. This results in the loss of the periodic pattern in the unperturbed region.

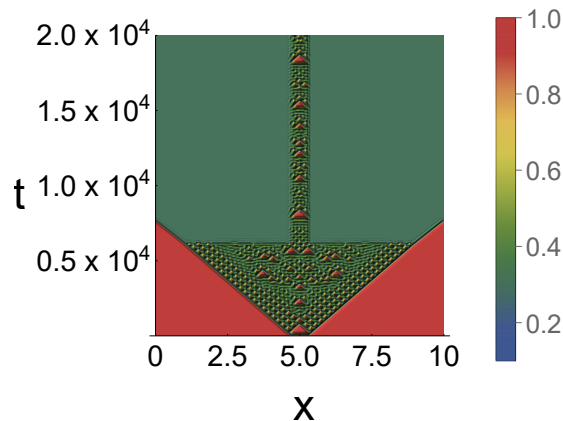


FIG. 8: Space-time plot where at  $t = 6,000$  we change in the 'perturbed' region the value of  $A$  from 0.0234 to 0.03, which drives that part of the system into the non-trivial steady state. This protocol, however, does not yield a periodic pattern in the 'unperturbed' region.

state, see Fig. 1. Clearly, periodic patterns are not emerging when patching together a chaotic region with a region that displays a steady state, i.e. when imposing on the chaotic region fixed boundary conditions that result from the adjacent steady-state region.

A zoom of the space-time pattern that results from using locally the time-delayed feedback scheme, see Fig. 9, reveals the formation of a transition region that straddles the boundary

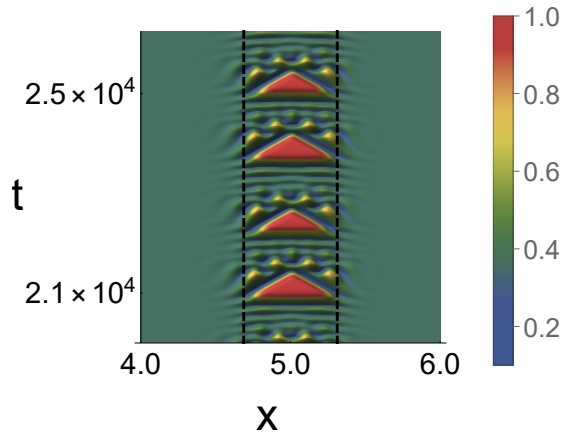


FIG. 9: A zoom into the periodic pattern from the left panel of Fig. 7 that reveals complex pattern in the perturbed part of the system close to the boundaries (indicated by the vertical dashed lines) with the unperturbed part. Without these features extending into the perturbed part, periodic pattern can not be established in the unperturbed region.

separating the perturbed and unperturbed regions. These features die out further away from the boundary which results in the local establishment of the homogeneous steady state. It is the presence of the diffusion term that, in conjunction with the time-delayed feedback, generates the formation of this transition region necessary for the emergence of periodic patterns with periods orders of magnitude larger than the delay time.

### B. $K > 0$

A second protocol for perturbing only part of the system is explored in Figs. 10 and 11. We choose the same parameter values as for the results presented above, with the one change that the strength  $K = 0.025$  is now positive. Using these parameter values for a time-delayed feedback control of the whole system, one observes that the system is pushed into the trivial steady state with  $(u, v) = (1, 0)$ . However, applying this scheme to only part of the system yields a very different behavior, as shown in Fig. 10. Whereas in the unperturbed region spatio-temporal chaos persists, in the *perturbed* region an approximate periodic pattern is established where successive maxima are separated by a time interval  $T \approx 440$ , which is three orders of magnitude larger than the delay time. One way to look at this pattern is a succession of pulses that are generated at both interfaces with the chaotic

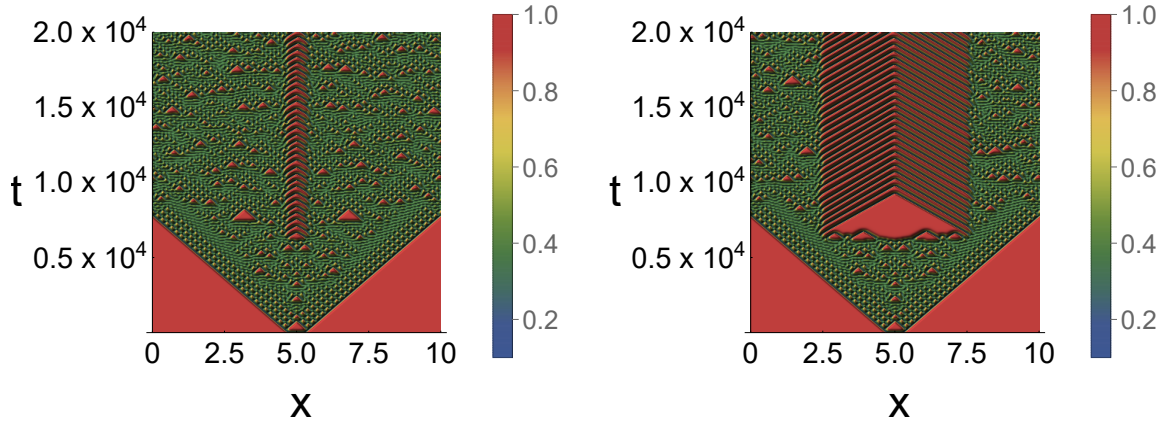


FIG. 10: Time-delayed feedback applied to only a part of the system with  $K > 0$  yields non-trivial patterns in the perturbed region, while spatio-temporal chaos persists in the unperturbed region. The values of the rates and of the delay time used for these panels are the same as for the panels in Fig. 2, with the exception of the strength which is  $K = 0.025$ . The width  $W$  of the perturbed region is  $W = 0.625$  in the left panel, while in the right panel half of the system is subjected to time-delayed feedback scheme.

regime, which acts as provider of a temporally fluctuating boundary condition. These pulses, after progressing through the perturbed region, undergo pair annihilation upon encounter. Inspection of the Fourier transform, see Fig. 11, reveals the imperfect oscillations in the form of a wide noisy peak at a frequency close to  $f = 0.0023$ , but the imperfect nature of the repeating pattern is also readily seen from the time-dependent species concentration shown in the inset.

The two panels in Fig. 10 differ by the width of the perturbed region. In fact, the approximate periodic pattern is observed for most widths, with the exception of very small regions ( $W \lesssim 0.3$ ), for which no persisting regular pattern can be established, and very large regions ( $L - W \lesssim 0.3$ ) which end up in the trivial steady state, similar to the fully controlled system. It follows that for this case the range of widths for which approximate periodic pattern emerge in the perturbed region scales linearly with the system size. The formation of this pattern needs a strength  $K > 0.015$ , as for very small  $K$  a regular pattern can not be stabilized and the system remains in the chaotic regime. For cases that result in the imperfect oscillations, the average time elapsed between successive maxima depends slightly on the value of  $K$ .

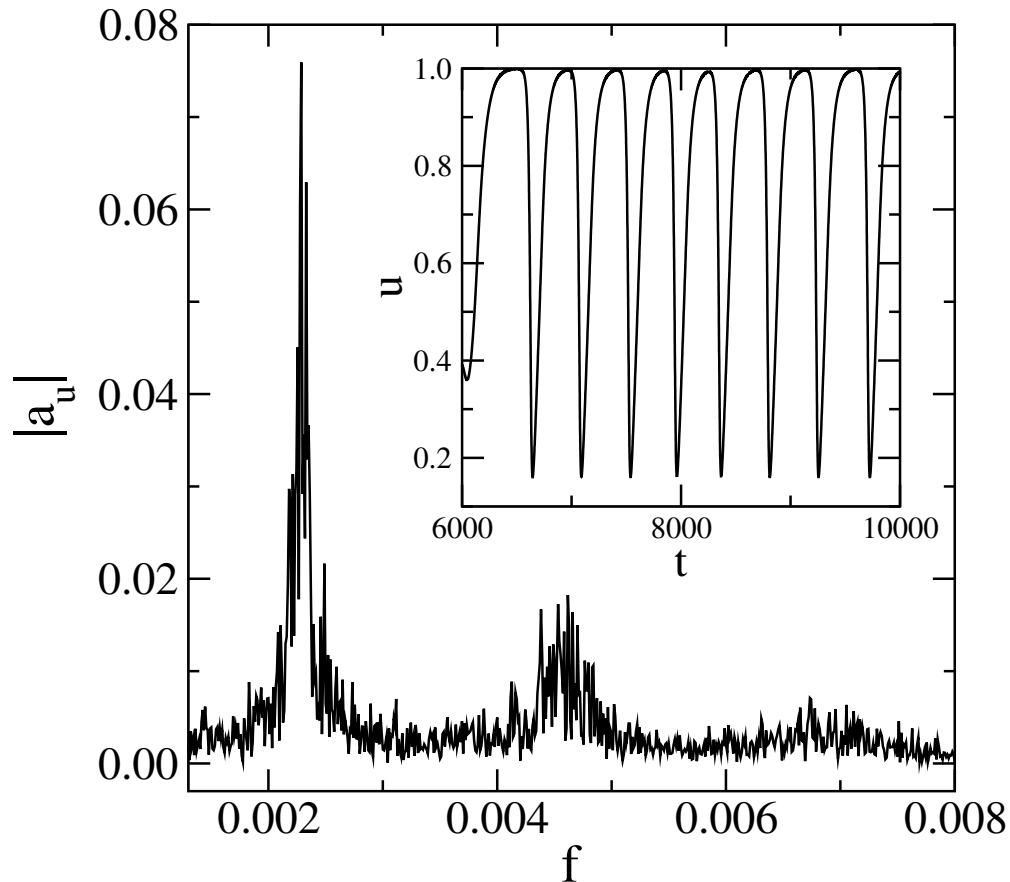


FIG. 11: Frequency-dependent amplitude of the Fourier transform of the time-dependent concentration  $u$  in the middle of the perturbed region, see the left panel in Fig. 10 for the corresponding space-time plot. The time series  $u(t)$  shown in the inset reveals an imperfect repeating pattern with successive maxima separated by a time interval  $T \approx 440$ .

#### IV. CONCLUSIONS AND OUTLOOK

Systems with transient chaos can be forced into different dynamic regimes through an external intervention. Protocols proposed for this include spatially arranged pinning sides as well as time-delayed feedback control. The latter method has been applied in the past [23] to the one-dimensional Gray-Scott model in order to generate other global dynamics.

In this work we have shown that applying time-delayed feedback to only part of the system may create novel spatially localized space-time pattern. We discussed two cases, one leading to perfect periodic pattern in the *unperturbed* part of the system, the other leading to imperfect oscillations in the perturbed region. The creation of these patterns turns out to be robust and is encountered for a broad range of system parameters. Our study reveals

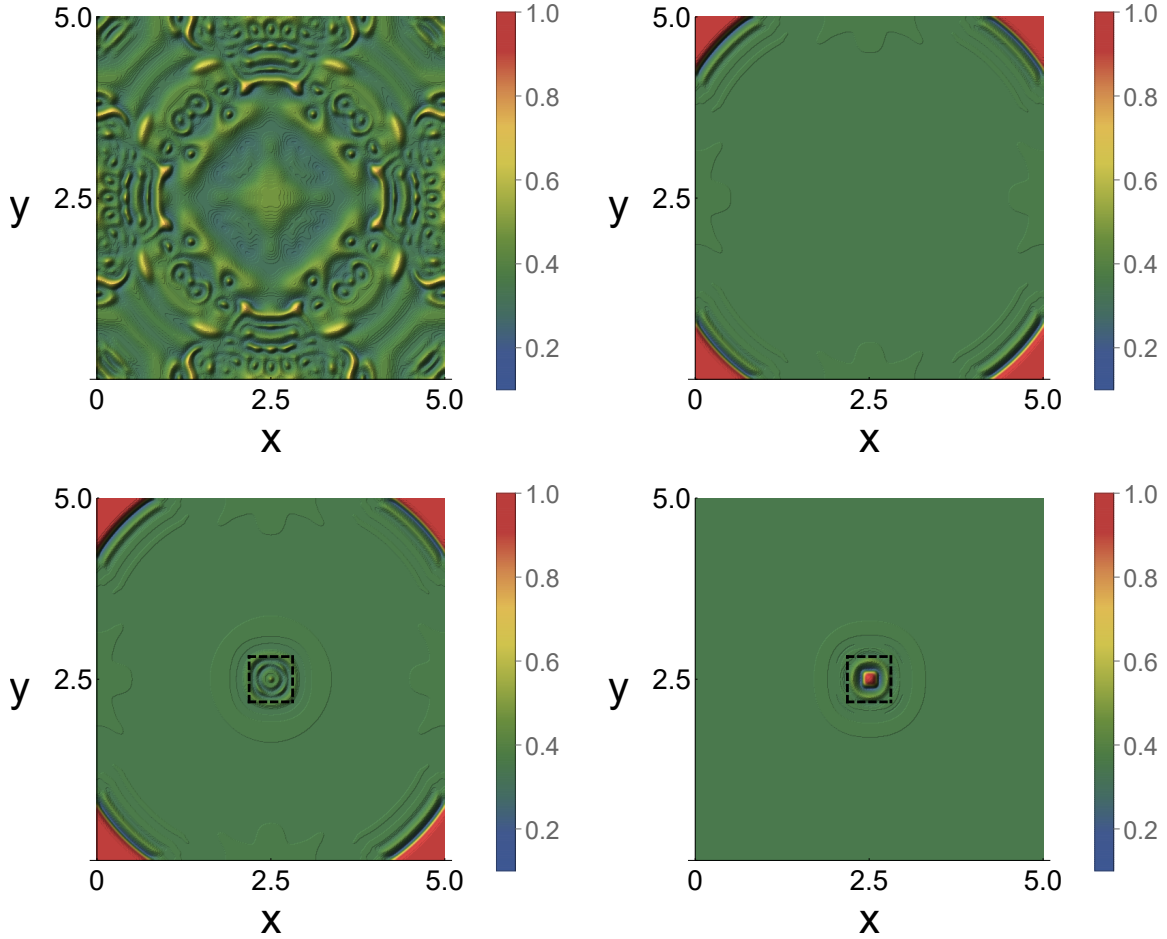


FIG. 12: Some snapshots for the two-dimensional Gray-Scott model with periodic boundary conditions and an inhomogeneous initial state with  $(u, v) = (0.5, 0.25)$  in a small square central region and  $(u, v) = (1, 0)$  everywhere else. The common parameters are  $A = 0.0238$  and  $B = 0.05$ , whereas the time increment is  $\Delta t = 0.05$ . (Top) The unperturbed system at  $t = 5,000$  (left) and the system subjected to global control with  $K = -0.25$  at  $t = 5,000$  (right). (Bottom) The system at  $t = 5,000$  (left) and at  $t = 18,750$  (right) for the case where, with the exception of a small square region of size  $0.3125 \times 0.3125$ , indicated by dashed lines, the system is subjected to spatially localized perturbation with strength  $K = -0.25$ . Both for global and spatially localized perturbations, time-delayed feedback is switched on at  $t = 250$ .

that the needed ingredient is the diffusion across the boundaries separating the perturbed and unperturbed regimes which yields a transition region, straddling the boundary, that is necessary to stabilize the spatially localized oscillations.

As shown in earlier work, in order to stabilize complex spatio-temporal dynamics near a

subcritical Hopf bifurcation using time-delayed feedback control, the delay time  $\tau$  has to be chosen as a multiple of the period of the periodic pattern to be stabilized [26–28]. This is very different from what we have discussed in this work as a local time-delayed perturbation stabilizes spatially localized patterns with periods orders of magnitude larger than the delay time. It is the interplay between time delay and boundaries separating perturbed and unperturbed regions that is the driving mechanism for the generation of these patterns with very long periods.

Our scheme is not restricted to the one-dimensional Gray-Scott model and similar results can be obtained in other situations as well as in other systems, including systems with truly chaotic behavior like the complex Ginzburg-Landau model [40]. Fig. 12 illustrates this for the two-dimensional Gray-Scott model where new patterns are locally created in the central region that is unperturbed. A detailed discussion of this situation will be presented elsewhere.

Time-delayed feedback has been used experimentally to stabilize unstable periodic orbits of chaotic systems [41–45], but we are not aware of an attempt to do this in a spatially localized way as discussed in this work. As we have shown, new spatially localized pattern can be stabilized through spatially localized time-delayed feedback. We hope that our work paves the way for experimental implementations of this scheme and for the investigation of the resulting spatially localized patterns.

### Acknowledgments

Research was sponsored by the Army Research Office and was accomplished under Grant No. **W911NF-17-1-0156**. The views and conclusions contained in this document are those of the authors and should not be interpreted as representing the official policies, either expressed or implied, of the Army Research Office or the U.S. Government. The U.S. Government is authorized to reproduce and distribute reprints for Government purposes notwithstanding any copyright notation herein.

---

[1] M. C. Cross and P. C. Hohenberg, *Rev. Mod. Phys.* **65**, 851 (1993).

- [2] D. Walgraef, *Spatio-Temporal Pattern Formation: With Examples from Physics, Chemistry, and Materials Science* (Springer, New York, 1997)
- [3] M. Matsushita, J. Wakita, H. Itoh, I. Ràfols, T. Matsuyama, H. Sakaguchi, and M. Mimura, *Physica A* **249**, 517 (1998).
- [4] H. Meinhardt, *Curr. Top. Dev. Biol.* **81**, 1 (2008).
- [5] F. X. Hu, G. X. Wu, G. X. Song, Q. R. Yuan, and S. Okamura, *Astrophys. Space Sci.* **302**, 43 (2006).
- [6] M. Einasto, L. J. Liivamägi, E. Tempel, E. Saar, E. Tago, P. Einasto, I. Enkvist, J. Einasto, V. J. Martínez, and P. Heinämäki, *Astrophys. J.* **736**, 51 (2011).
- [7] A. De Wit, *Adv. Chem. Phys.* **109**, 435 (1999).
- [8] A. M. Turing, *Phil. Trans. R. Soc. B* **237**, 37 (1952).
- [9] P. Gray and S. K. Scott, *Chemical Oscillations and Instabilities: Non-linear Chemical Kinetics* (Oxford University Press, Oxford, 1990).
- [10] Y.-C. Lai and T. Tél, *Transient Chaos: Complex Dynamics on Finite Timescales in Applied Mathematical Sciences Vol. 173* (Springer, New York, 2011).
- [11] J. Wolff, A. G. Papathanasiou, H. H. Rotermund, G. Ertl, X. Li, and I. G. Kevrekidis, *Phys. Rev. Lett.* **90**, 018302 (2003).
- [12] V. S. Zykov, G. Bordiougov, H. Brandtstädter, I. Gerdes, and H. Engel, *Phys. Rev. Lett.* **92**, 018304 (2004).
- [13] A. S. Mikhailov and K. Showalter, *Phys. Rep.* **425**, 79 (2006).
- [14] V. K. Vanak and I. R. Epstein, *Chaos* **18**, 026107 (2008).
- [15] S. V. Gurevich, *Phys. Rev. E* **87**, 052922 (2013).
- [16] J. Löber and H. Engel, *Phys. Rev. Lett.* **112**, 148305 (2014).
- [17] H. Nakao, T. Yanagita, and Y. Kawamura, *Phys. Rev. X* **4**, 021032 (2014).
- [18] E. Ott, C. Grebogi, and J. A. Yorke, *Phys. Rev. Lett.* **64**, 1196 (1990).
- [19] K. Pyragas, *Phys. Lett. A* **170**, 421 (1992).
- [20] M. E. Bleich and J. E. S. Socolar, *Phys. Rev. E* **54**, R17 (1996).
- [21] S. Boccaletti, C. Grebogi, Y.-C. Lai, H. Mancini, and D. Maza, *Phys. Rep.* **329**, 103 (2000).
- [22] E. Schöll and H. G. Schuster (Editors), *Handbook of Chaos Control: Foundations and Applications* (Wiley-VCH, Weinheim, 2008).
- [23] Y. N. Kyrychko, K. B. Blyuss, S. J. Hogan, and E. Schöll, *Chaos* **19**, 043126 (2009).

- [24] A. L. Fradkov, *Phil. Trans. R. Soc. A* **375**, 20160223 (2017).
- [25] R. O. Grigoriev, M. C. Cross, and H. G. Schuster, *Phys. Rev. Lett* **79**, 2795 (1997).
- [26] B. Fiedler, V. Flunkert, M. Georgi, P. Hövel, and E. Schöll, *Phys. Rev. Lett.* **98**, 114101 (2007).
- [27] M. Kehrt, P. Hövel, V. Flunkert, M. A. Dahlem, P. Rodin, and E. Schöll, *Eur. Phys. J. B* **68**, 557 (2009).
- [28] G. Brown, C. M. Postlethwaite, and M. Silber, *Physica D* **240**, 859 (2011).
- [29] P. Gray and S. K. Scott, *Chem. Eng. Sci.* **39**, 1087 (1994).
- [30] W. N. Reynolds, J. E. Pearson, and S. Ponce-Dawson, *Phys. Rev. Lett.* **72**, 2797 (1994).
- [31] W. Mazin, K. E. Rasmussen, E. Mosekilde, P. Borckmans, and G. Dewel, *Math. Comput. Simul.* **40**, 371 (1996).
- [32] Y. Nishiura and D. Ueyama, *Forma* **15**, 281 (2000).
- [33] Y. Nishiura and D. Ueyama, *Physica D* **150**, 137 (2001).
- [34] I. Berenstein, *Chaos* **25**, 064301 (2015).
- [35] P. Gandhi, Y. R. Zelnik, and E. Knobloch, *Phil. Trans. R. Soc. A* **376**, 20170375 (2018).
- [36] J. E. Pearson, *Science* **261**, 189 (1993).
- [37] C. B. Muratov and V. V. Osipov, *Eur. Phys. J. B* **22**, 213 (2001).
- [38] F. Lesmes, D. Hochberg, F. Morán, and J. Pérez-Mercader, *Phys. Rev. Lett.* **91**, 238301 (2003).
- [39] Of course, this can be generalized to other control schemes as for example control of the reactant  $V$  through time-delayed feedback control.
- [40] J. Czak and M. Pleimling, in preparation.
- [41] K. Pyragas and A. Tamaševičus, *Phys. Lett. A* **180**, 99 (1993).
- [42] W. Just, E. Reibold, and H. Brenner, in *Proceedings of the 5th Experimental Chaos Conference*, edited by M. Ding, W. L. Ditto, L. M. Pecora, and M. L. Spano, 67 (2001).
- [43] O. V. Popovych, C. Hauptmann, and P. A. Tass, *Phys. Rev. Lett.* **94**, 164102 (2005).
- [44] K. Yamasue, K. Kobayashi, H. Yamada, K. Matsushige, and T. Hikihara, *Phys. Lett. A* **373**, 3140 (2009).
- [45] T. Jüngling, A. Gjurchinovski, and V. Urumov, *Phys. Rev. E* **86**, 046213 (2012).